Contrib. Plasma Phys. **54**, No. 8, 697 – 711 (2014) / **DOI** 10.1002/ctpp.201300060

Self-Force in 1D Electrostatic Particle-in-Cell Codes for Non-Equidistant Grids

J. Duras[1]*, **K. Matyash**[2]**, **D. Tskhakaya**[3,4]***, **O. Kalentev**[1]†, and **R. Schneider**[1]‡

[1] Institute of Physics, Ernst-Moritz-Arndt University of Greifswald, Felix-Hausdorff-Str. 6, D-17487 Greifswald, Germany
[2] Computing Centre, Ernst-Moritz-Arndt University of Greifswald, Felix-Hausdorff-Str. 12, D-17489 Greifswald, Germany
[3] Permanent address: Andronikashvili Institute of Physics, 0177 Tbilisi, Georgia
[4] Association Euratom-AW, Institute of Applied Physics, TU Wien, A-1040 Vienna, Austria

Received 18 October 2013, revised 19 November 2013, accepted 21 November 2013
Published online 24 February 2014

Key words Electrostatic Particle-in-Cell, Self-force, non-uniform grid.

Effects of non-equidistant grids on momentum conservation is studied for simple test cases of an electrostatic 1D PIC code. The aim is to reduce the errors in energy and momentum conservation. Assuming an exact Poisson solver only numerical errors for the particle mover are analysed. For the standard electric field calculation using a central-difference scheme, artificial electric fields at the particle position are generated in the case when the particle is situated next to a cell size change. This is sufficient to destroy momentum conservation. A modified electric field calculation scheme is derived to reduce this error. Independent of the calculation scheme additional fake forces in a two-particle system are found which result in an error in the total kinetic energy of the system. This contribution is shown to be negligible for many particle systems. To test the accuracy of the two electric field calculation schemes numerical tests are done to compare with an equidistant grid set-up. All tests show an improved momentum conservation and total kinetic energy for the modified calculation scheme of the electric field.

1 Introduction

Particle-in-Cell (PIC) codes are standard tools for plasma simulations [1]. They follow the kinetics of charged particles in a system and calculate the fields self-consistently on a spatial grid in order to reduce the computational costs. The accuracy of this method is determined, among others, by the grid cell size. The grid has to resolve locally the smallest length scale. Usually, this is the electron Debye length. In addition, special geometries of physical boundaries can require a finer grid in order to resolve boundaries accurately. These restrictions of the cell size strongly limits the computationally possible size of the simulation domain.

To simulate larger domains to resolve special geometries different mesh generation strategies like Boundary-Fitted Coordinates (BFC) [2] or Adaptive Mesh Refinement (AMR) [3], have been used. Non-uniform grids often lead to non-trivial interpolation functions [4] and a strong change in cell size can cause non-physical effects, for example self-forces. Therefore, many of these applied methods are not momentum conserving.

A first approach for an electrostatic PIC code with a non-uniform grid avoiding self-forces was given by Fichtl [5]. Colella et al. made some effort to estimate the error caused by a non-equidistant grid [6].

In this paper momentum and kinetic energy conservation for a 1D electrostatic PIC code using non-equidistant grids is analysed. Such conservation is equivalent to the non-existence of self-forces and correct inter-particle interactions. The outline of the paper is as follows: After a short description of the general PIC cycle, constraints

* Corresponding author. E-mail: durasj@uni-greifswald.de
** E-mail: knm@ipp.mpg.de
*** E-mail: david.tskhakaya@uibk.ac.at
† E-mail: okalenty@ipp.mpg.de
‡ E-mail: schneider@uni-greifswald.de

for momentum conservation, weighting function and Green's function are derived for non-uniform grids. In the following is shown that even for an exact Poisson solver the calculation scheme for the electric field can introduce errors destroying momentum conservation. For simplicity a system of a single particle in a 1D electrostatic PIC code is destroying. It will be shown that for a non-equidistant grid the two-point central difference scheme used for the electric field calculation generates self-forces to minimize this non-physical force a modified electric field calculation is presented. For the modified field calculation as well as for the conservative one, the error in the total kinetic energy is derived. Since PIC is not conserving energy, this derivation is done to prove that no additional forces are appearing. Within single-particle and two-particle set-ups total kinetic energy and momentum conservation are tested numerically and compared with an equidistant grid case.

2 General scheme of electrostatic PIC

The Particle-in-Cell method calculates the time evolution of a plasma in so-called PIC cycles, where potential and electric field are calculated at grid points based on the electric field calculated from the charges of pseudo particles, representing a bunch of physical particles. These are pushed using the electric field calculated before. The simplest grid is an equidistant grid, where each cell has the same quadratic size $\Delta\mathbf{x} = (\Delta x, \Delta x, \Delta x)^T$. A non-equidistant grid has cells with different size $\Delta\mathbf{x}_i \neq \Delta\mathbf{x}_j$, where $\Delta\mathbf{x}_i = (\Delta x_i, \Delta y_i, \Delta z_i)^T$, but not necessarily for each cell.

To solve the Poisson equation the charge density is needed at the grid points. For a system with $i = 0, ..., N_g$ grid points, the charge density is calculated as

$$\rho_i = \frac{q_i}{\nu_i} \,, \tag{1}$$

where ν_i is the corresponding cell volume and q_i the collective charge assigned to the grid point. For this "grid point charge", a weighting function W interpolates the particle charge Q_p from the particle position $\mathbf{X}_p$ to the grid point position $\mathbf{x}_i$

$$q_i = \sum_{p=1}^{N_p} Q_p \cdot W(\mathbf{X}_p, \mathbf{x}_i) \,. \tag{2}$$

N_p is the number of charged particles in the system. With the resulting charge density ρ_i on the grid, the electric field given by the field equation

$$\nabla \cdot \mathbf{E} = \frac{1}{\varepsilon_0}\rho \,, \tag{3}$$

can be calculated on the grid. In PIC codes, this is done in two steps. At first, the Poisson equation

$$\nabla^2\phi = -\frac{1}{\varepsilon_0}\rho \tag{4}$$

is solved numerically for the electric potential ϕ_i at the grid points x_i. Afterwards, the electric field at the grid point E_i is calculated by

$$\mathbf{E} = -\nabla\phi \,, \tag{5}$$

to solve the equation of motion for each pseudo particle $p = 1, ..., N_p$

$$\dot{\mathbf{V}}_p = \frac{Q_p}{m_p}(\mathbf{E}(\mathbf{X}_p) + \mathbf{V}_p \times \mathbf{B})$$

located in the domain, with mass m_p and velocity $\mathbf{V}_p$. For simplicity we consider a constant magnetic field $\mathbf{B}$. The electric field values $\mathbf{E}(\mathbf{X}_p)$ have to be interpolated from grid points to particle positions $\mathbf{X}_p$. This is done by a weighting function W'

$$\mathbf{E}(\mathbf{X}_p) = \sum_{i=0}^{N_g} \mathbf{E}_i \cdot W'(\mathbf{X}_p, \mathbf{x}_i) \,. \tag{6}$$

This defines the current velocity of the particle $\mathbf{V}_p = \mathbf{V}_p(t)$ and allows to calculate the a new position of the particle at the next time step $\mathbf{X}_p(t + \Delta t) = \mathbf{X}_p(t) + \mathbf{V}_p(t) \cdot \Delta t$. The equation of motion is solved with the so-called pusher. Boundary conditions of the domain have to be taken into account. At the end of the PIC cycle, collisions can be introduced by Monte Carlo methods. For the next time step, the particle charges need to be interpolated on the grid points and the PIC cycle is repeated.

To analyse the total numerical error of a complete PIC cycle, one has to derive the overall error in the forces $\mathbf{F}(\mathbf{X}_p) = Q_p\mathbf{E}(\mathbf{X}_p)$ acting on each particle. This is determined by weighting functions, Poisson Solver and particle pusher. These different contributions interact with each other and therefore have to fulfil both individually and in their combination charge, energy and momentum conservation [1].

In this paper the performance and the interaction of the different numerical contributions with respect to the generation of a non-physical self-force will be investigated. For a better understanding of the problem a 1D system is considered.

2.1 Momentum conservation

Momentum conservation in PIC is determined by Newton's third law of motion. The force F_{12} acting on a charged particle 1 generated by the electric field of a charged particle 2 has to act opposite to the force F_{21} acting on particle 2 generated by the electric field of particle 1

$$F_{12} = -F_{21} \ . \tag{7}$$

With the help of a discrete Green's function $\hat{g}(x_i, x_k)$, defined at grid points $i, k = 0, ..., N_g$, the electric field can be expressed as

$$E_i = \frac{1}{\varepsilon_0} \sum_{k=0}^{N_g} \hat{g}(x_i, x_k) q_k \ , \tag{8}$$

as given by Hockney [1]. The Green's function element $\hat{g}(x_i, x_k) = g_{ik}$ corresponds to the electric field at the grid point x_i generated by the charge corresponding to the grid point x_k. Therefore, the force on particle 1, located at spatial coordinate X_1, due to particle 2 at spatial coordinate X_2, is given by equation 2, 6 and 8 as

$$F_{12} = \frac{Q_2 Q_1}{\varepsilon_0} \sum_{i,k} W(X_2, x_i,) \hat{g}(x_i, x_k) W'(X_1, x_k) \ . \tag{9}$$

Vice versa, the force on particle 2, generated by particle 1 is

$$F_{21} = \frac{Q_1 Q_2}{\varepsilon_0} \sum_{i,k} W(X_1, x_k) \hat{g}(x_k, x_i) W'(X_2, x_i) \ . \tag{10}$$

The special case of an equidistant grid can be found in [1]. To fulfil equation 7, two constraints have to be fulfilled. The first is to have the same weighting function for assigning the charge from the particles onto the grid (W) and to interpolate the electric field from the grid back to the particles' positions (W'):

$$W(x, y) = W'(x, y). \tag{11}$$

The second constraint is the antisymmetry of the Green's function

$$\hat{g}(x_i, x_k) = -\hat{g}(x_k, x_i) \quad \forall i, k \ . \tag{12}$$

In this paper the influence of a non-equidistant grid on the antisymmetry of the Green's function is studied. Therefore, condition equation 11 is assumed to be fulfilled.

3 Error in Green's function

An analytical 1D Green's function of a PIC code with non-equidistant grid was given by Tskhakaya at al [7]. Here, each cell has an individual size Δx_i. Integration of the 1D Poisson equation using the Gauss theorem gives

$$E(x_i) = \frac{1}{2\varepsilon_0}\left(\int_{x_0}^{x_i} \rho\, dx - \int_{x_i}^{x_{N_g}} \rho\, dx\right) ,$$

for the absence of external fields. The integrals can be approximated with the Trapezoidal rule

$$E(x_i) = \frac{1}{2\varepsilon_0}\left(\sum_{k=0}^{i-1} \frac{\Delta x_k}{2}(\rho_k + \rho_{k+1}) - \sum_{k=i+1}^{N_g-1} \frac{\Delta x_k}{2}(\rho_k + \rho_{k+1})\right)$$

Assuming charges to be mapped on grid centers, in 1D the volume corresponding to the charge density ρ_i is defined as $\nu_i = \Delta x_i \ \forall i = 1, ..., N_g - 1$ and for the boundary cells of the domain as $\nu_0 = 0.5\Delta x_0$ and $\nu_{N_g} = 0.5\Delta x_{N_g-1}$. Therefore the Green's function as defined in equation 8 is given as

$$\hat{g}(x_i, x_k) = g_{ik} = \begin{cases} +\frac{1}{2} & \text{if } i > k \\ \frac{1}{4}\frac{\Delta x_{i-1} - \Delta x_i}{\Delta x_{i-1} + \Delta x_i} & \text{if } i = k \\ -\frac{1}{2} & \text{if } i < k \end{cases} .$$

The different scaling of g_{ik} compared to [7] originates from its definition corresponding to the collective charge instead of charge density. One can see, that the antisymmetry is not violated for $i \neq k$. But for $i = k$, diagonal elements $\hat{g}(x_i, x_i) = g_{ii}$ are non-zero, if the neighbouring cells have different sizes $\Delta x_{i-1} \neq \Delta x_i$. The antisymmetry is broken. As given by equation 8, the diagonal element is the proportionality factor to calculate the electric field at a grid point x_i generated by the charge associated with that grid point

$$E_i = g_{ii} q_i .$$

For a $g_{ii} \neq 0$, the charge experiences a non-physical self-force $F_{self} = q_i E_i \neq 0$. Therefore, broken antisymmetry of the Green's function results in violation of momentum conservation, if charge is associated with a grid point of different sized neighbouring cells.

In the electrostatic plasma assumption the Green's function is defined by the differential equation 3 and therefore by the differential operator ∇. In the PIC code itself, the differential equation is realized by a discrete calculation, namely numerical approximations of the Poisson equation 4 and the electric field calculation equation 5. If the two calculations have the same solution as the analytic equation 3, the numerical schemes are exact and the Green's function is antisymmetric. But if the numerical schemes differ from the analytic solution, antisymmetry is no longer ensured and violation of momentum conservation is possible. Here, the interaction of Poisson solver and electric field calculation is important because approximation errors in the individual steps can be annihilated or amplified.

For simplicity, an exact Poisson solver is assumed in this work. Therefore, the influence of a non-equidistant grid on the antisymmetry of the Green's function is reduced to the numerical calculation scheme of the electric field. To analyse the generation of a self force, an analytical test case of a single pseudo particle in its own field, located at the grid point $x_p = X_p$, is used. That means, only one grid point is associated with charge. The boundary conditions of the computational domain for a single particle in its own field are

$$E_0 = -E_{N_g} ,$$

where E_0 and E_{N_g} denotes the values of the electric field at the first and the last grid point of the domain. In 1D the resulting potential is linear, as sketched in Fig. 1. It can be interpreted as the potential of a charged sheath infinite in y and z directions, but infinite small in x direction.

In the following the accuracy of the calculation scheme for the electric field is analysed for a non-equidistant grid.

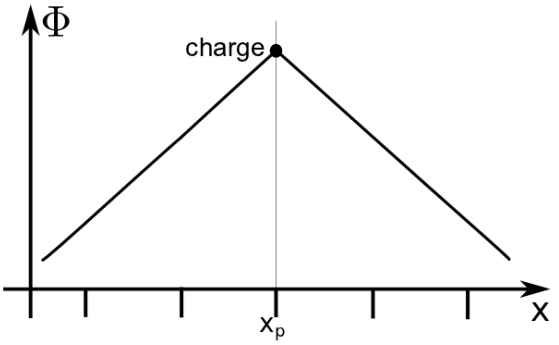

Fig. 1 1D Potential of a charged particle located at $X_p = x_p$.

3.1 Electric field calculation

In the case of an equidistant grid the calculation of the electric field in an electrostatic 1D PIC code is typically done by a two-point central difference scheme. For a non-equidistant grid, it becomes

$$E_i = -\frac{\phi_{i+1} - \phi_{i-1}}{\Delta x_{i-1} + \Delta x_i} \ . \tag{13}$$

This scheme is also applicable for higher dimensional approaches, where it is used for each coordinate. To study its accuracy, the two different regions of the potential, the differentiable region $x_i \neq x_p$ and the particle position x_p, can be analysed separately. At first, it will be proven that E_i is exact for the differentiable region of the potential.

For all grid points in the piecewise linear parts of the potential $x_i \neq x_p$, its accuracy is given by a Taylor series expansion of $\phi(x_{i-1})$ and $\phi(x_{i+1})$ around x_i. One gets

$$\frac{\phi_{i+1} - \phi_{i-1}}{\Delta x_{i-1} + \Delta x_i} = \left.\frac{\mathrm{d}\phi}{\mathrm{d}x}\right|_{x_i} + \sum_{k=2}^{\infty} \left.\frac{\mathrm{d}^k\phi}{\mathrm{d}x^k}\right|_{x_i} \frac{\Delta x_i^k - (-\Delta x_{i-1})^k}{k!(\Delta x_i + \Delta x_{i-1})} \quad \forall x_i \neq x_p \ ,$$

where the sum represents the error of the calculation scheme. Since the right hand side of the Poisson equation (4) is zero for all $x_i \neq x_p$, also the second derivative of the potential at x_i is zero. Therefore, all higher derivatives are zero as well and the error vanishes. The two-point central difference scheme is exact for all grid points $x_i \neq x_p$. Therefore, the corresponding entries of the Green's function are antisymmetric $g_{ik} = -g_{ki} \ \ \forall i \neq k$, as shown in the section before.

At the particle grid point the potential has a discontinuity, therefore the Taylor series around x_p is not defined. To determine the accuracy, the symmetry of the potential around x_p can be used. To ensure condition equation (12) to avoid self forces, E_p has to be zero. For neighbouring cells of the same size $\Delta x_{i-1} = \Delta x_i$, the potential ϕ_{i+1} and ϕ_{i-1} have the same values and the electric field is

$$E_p = \frac{\phi_{p+1} - \phi_{p-1}}{2\Delta x_{p-1}} = 0 \quad \text{for} \ \ \Delta x_{p-1} = \Delta x_p \ .$$

No self force is generated. But if $\Delta x_{i-1} \neq \Delta x_i$, the potential values are not equal and the resulting electric field differs from zero

$$E_p = \frac{\phi_{p+1} - \phi_{p-1}}{\Delta x_{p-1} + \Delta x_p} \neq 0 \quad \text{for} \ \ \Delta x_{p-1} \neq \Delta x_p \ .$$

This artificial electric field affects the particle as a self-force, although the calculated potential is correct. The diagonal elements of the Green's function corresponding to the a change of cell size are $g_{ii} \neq 0 \ \forall \Delta x_i \neq \Delta x_{i-1}$. The antisymmetry is broken and momentum conservation is violated.

To overcome this violation a calculation scheme has to be found which ensures antisymmetry of the Green's function for all grid points. In the next section a modified calculation scheme E_i' is derived.

4 A modified electric field calculation

To illustrate the source of error in the typical electric field calculation in a non-equidistant grid and the idea of the modified calculation scheme, the 1D system is used. In Fig. 2a and 2b, the potential of a single particle located at a grid point x_p, with neighbouring grid cells of different size $\Delta x_{p-1} < \Delta x_p$ is shown. The values of the potential on the grid points ϕ_i are marked by a black dot, while the black line represents the analytic solution of ϕ. Since the Poisson solver is assumed to be exact, the dots lie on the line. For the conservative and the modified calculation scheme, the electric field at x_p is given by the slope of the red dashed line, respectively of the blue dot-dashed line.

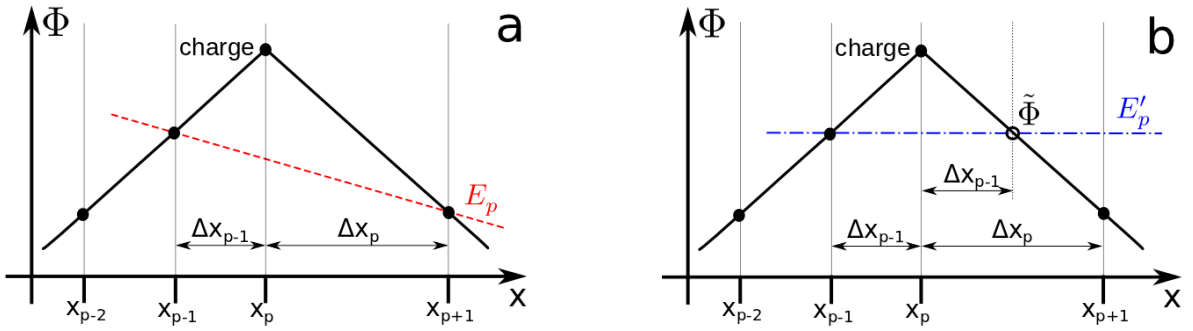

Fig. 2 Electric field calculation for a charged particle located at x_p, in an non-equidistant grid with a change of cell size $\Delta x_{p-1} \neq \Delta x_p$. a: Calculation scheme E_p as for an equidistant grid. b: Modified field calculation E'_p.

While the usual calculation scheme is a two-point central difference scheme equation (13), E_p in Fig. 2a is non zero and therefore wrong. One can see, that the field inaccuracy has its origin in the unsymmetrical positions of the used neighboring potential values ϕ_{p-1} and ϕ_{p+1} appearing due to the different cell sizes. The idea of the corrected calculation for a non-equidistant grid is restore the spatial symmetry in the derivation scheme. Therefore, instead of $\phi_{p+1} = \phi(x_p + \Delta x_p)$, an approximated value $\tilde{\phi} \approx \phi(x_p + \Delta x_{p-1})$ is used. The two point central difference scheme gets

$$E'_i = \begin{cases} -\dfrac{\phi_{i+1} - \phi_{i-1}}{2\Delta x_{i-1}} & \text{if } \Delta x_{i-1} = \Delta x_i \\ -\dfrac{\tilde{\phi} - \phi_{i-1}}{2\Delta x_{i-1}} & \text{if } \Delta x_{i-1} \neq \Delta x_i \end{cases} . \tag{14}$$

For the system of a single particle at grid point x_p, a linear interpolation between the neighbouring points gives the exact solution for

$$\tilde{\phi} := \phi_p(1 - \frac{\Delta x_{p-1}}{\Delta x_p}) + \phi_{p+1}\frac{\Delta x_{p-1}}{\Delta x_p} = \phi(x_p + \Delta x_{p-1}) . \tag{15}$$

In Fig. 2b $\tilde{\phi}$ is the key element for the correction. Hence $E'_p = E(x_p)$ gives the correct analytical value, as shown by the slope of the blue dot-dashed line.

This modified calculation scheme can also be derived differently. For the single particle system, the potential is piecewise linear, but has a discontinuity in the first derivative at the particle position X_p. That means that the derivative of the potential at this point is not defined. Therefore, also the electric field at this point is not defined. But since for all position to the left and to the right of X_p the potential is continuously differentiable, right-sided and left-sided derivatives at the particle position are defined as

$$\left.\frac{\mathrm{d}\phi}{\mathrm{d}x}\right|^r_{X_p} := \lim_{\eta\to 0}\frac{\phi(X_p) - \phi(X_p - \eta)}{\eta}$$
$$\left.\frac{\mathrm{d}\phi}{\mathrm{d}x}\right|^l_{X_p} := \lim_{\eta\to 0}\frac{\phi(X_p + \eta) - \phi(X_p)}{\eta} ,$$

with $\eta \in \mathbb{R}^{>0}$. For a 1D system of a single charge, the one-sided derivatives give $\frac{\mathrm{d}\phi}{\mathrm{d}x}\Big|_{X_p}^{r} = -E$ and $\frac{\mathrm{d}\phi}{\mathrm{d}x}\Big|_{X_p}^{l} = +E$, with the analytical value of the electric field $E = const$, generated by the particle.

Although mathematically the electric field at the particle position is not defined, the physics requirement of non-existence of self-force requires $E(X_p)$ to be zero in a system of a single particle in its own field. While for this system the electric field to the left and to the right of the particle position has the same value but opposite sign, the analytical calculation of the electric field at X_p can be defined by the average of left-sided and right-sided derivatives

$$\mathcal{E}(X_p) := -\frac{\frac{\mathrm{d}\phi}{\mathrm{d}x}\Big|_{X_p}^{r} + \frac{\mathrm{d}\phi}{\mathrm{d}x}\Big|_{X_p}^{l}}{2} = \lim_{\eta\to 0} \frac{E(X_p-\eta) + E(X_p+\eta)}{2} \ . \tag{16}$$

For a single particle this definition gives an electric field value of 0 at X_p.

$$\begin{aligned}\mathcal{E}(X_p) &= \lim_{\eta\to 0} -\frac{1}{2}\left(\frac{\phi(X_p)-\phi(X_p-\eta)}{\eta} + \frac{\phi(X_p+\eta)-\phi(X_p)}{\eta}\right) \\ &= \lim_{\eta\to 0} -\frac{\phi(X_p+\eta)-\phi(X_p-\eta)}{2\eta} \ = \lim_{\eta\to 0} -\frac{0}{2\eta} \ \to 0\end{aligned}$$

Here, the symmetry of the potential $\phi(X_p-\eta) = \phi(X_p+\eta)\ \forall\eta \in \mathbb{R}^{>0}$ is used. This definition of the electric field is also valid for the smooth parts of the potential $X \neq X_p$, since right-sided derivatives and left-sided derivatives gives the same value $\frac{\mathrm{d}\phi}{\mathrm{d}x}\Big|_{X}^{r} = \frac{\mathrm{d}\phi}{\mathrm{d}x}\Big|_{X}^{l} \equiv \frac{\mathrm{d}\phi}{\mathrm{d}x}\Big|_{X}$. Therefore, equation (16) applied on X is equivalent to $\mathcal{E}(X) = -\frac{\mathrm{d}\phi}{\mathrm{d}x}\Big|_{X}\ \forall X \neq X_p$. From this analytic definition, the modified electric field calculation scheme can be derived. A discrete form of equation (16) is

$$\mathcal{E}(x_i) = \frac{E(x_i - \Delta x_{i-1}/2) + E(x_i + \Delta x_i/2)}{2} \quad \forall i = 1, ..., N_g - 1 \ . \tag{17}$$

For any isotropic system containing a single charged particle, this form gives the exact value as in equation (16). Since the general two point central difference scheme (13) is exact for all $x_i \neq x_p$ also

$$\begin{aligned}E(x_i - \Delta x_{i-1}/2) &= -\frac{\phi(x_i)-\phi(x_{i-1})}{\Delta x_{i-1}} \\ E(x_i + \Delta x_i/2) &= -\frac{\phi(x_{i+1})-\phi(x_i)}{\Delta x_i} \ ,\end{aligned}$$

is exact and can be used in equation (17). This gives the modified calculation scheme

$$E'_i = \mathcal{E}(x_i) = -\frac{\Delta x_{i-1}\phi_{i+1} + (\Delta x_i - \Delta x_{i-1})\phi_i - \Delta x_i \phi_{i-1}}{2\Delta x_i \Delta x_{i-1}} \ , \tag{18}$$

which is equivalent to equation (14) and equation (15).

To ensure antisymmetry of the Green's function equation (12), $E'_i = -\frac{\mathrm{d}\phi}{\mathrm{d}x}\Big|_{x_i}\ \forall i \neq p$ and $E'_p = 0$ has to be shown for the analytical test system. Since the electric field to the right and to the left of x_p is constant, $E(x_i) = -E$ for $i < p$ and $E(x_i) = +E$ for $i > p$, the potential is given by

$$\begin{aligned}\phi_{p-k} &= \phi_p - (x_p - x_{p-k}) \cdot E \\ \phi_{p+k} &= \phi_p - (x_{p+k} - x_p) \cdot E\end{aligned}$$

for $k \in \mathbb{N}^{>0}$. With this expressions and for a grid point $x_i > x_p$ equation (18) gets

$$\begin{aligned}E'_{i,i>p} &= -\frac{(\Delta x_{i-1} - \Delta x_i)(\phi_p - \phi_p + (x_p - x_i)\cdot E)}{2\Delta x_i \Delta x_{i-1}} + E \\ &= E \quad \forall \Delta x_i,\ \Delta x_{i-1} \ .\end{aligned}$$

Using the same procedure $E'_{i,i<p} = E$ can be shown. Therefore, the requirement $E'_i = -\frac{\mathrm{d}\phi}{\mathrm{d}x}\Big|_{x_i}\ \forall i \neq p$ is fulfilled. For the particle position x_p the same calculation gives:

$$E'_p = 0 \quad \forall \Delta x_p,\, \Delta x_{p-1}\ .$$

The modified calculation scheme for the electric field equation (18) is therefore exact for all grid points in a 1D system of a single charge with non-equidistant grid as well as for an equidistant grid and does not generate self forces. While also the calculated potential is assumed to be exact for all grid points, the Greens function is antisymmetric and the momentum is conserved. Instead of changing the electric field calculation it is also possible to prevent generation of self forces by modifying the weighting function W' as following

$$W'(X_p, x_i, \phi) = W(X_p, x_i) \cdot \frac{\Delta x_{i-1}\Delta^+\phi_{i+1} - \Delta^+\Delta^-\phi_i - \Delta x_i \Delta^+\phi_{i-1}}{2\Delta x_i \Delta x_{i-1}(\phi_{i+1} - \phi_{i-1})}\ ,$$

with $\Delta^+ := \Delta x_i + \Delta x_{i-1}$ and $\Delta^- := \Delta x_i - \Delta x_{i-1}$.

5 Consequences for energy conservation

Momentum conservation does not guarantee energy conservation, too. Since the equation is solved only at grid points the electric field at particle positions is an approximation and therefore the potential energy of the particle is also not correct. PIC does not conserve energy. In order to prove that not additional error is generated, we compare the kinetic energy obtained from the simulation with the corresponding analytical values.

If a particle "p" with charge Q_p and mass m_p at position $X_p \in [x_p; x_{p+1}]$ is assumed, its kinetic energy is given by $\mathcal{W}_p = 0.5\, m_p V_p^2$ and its kinetic energy change per unit time is

$$\frac{\mathrm{d}\mathcal{W}_p}{dt} = V_p Q_p (E + \frac{V_p \times B}{B^2})\,,$$

where E and B are the electric and magnetic field values at the particle position X_p. Therefore, the numerical error in the energy change per unit time for an electrostatic system is given by

$$\begin{aligned}\delta W_p &:= \frac{\mathrm{d}\mathcal{W}_p^{PIC}}{\mathrm{d}t} - \frac{\mathrm{d}\mathcal{W}_p^{an}}{\mathrm{d}t} = V_p Q_p \left(E(X_p)^{PIC} - E(X_p)^{an}\right) \\ &= V_p Q_p \sum_{i=0}^{N_g} W(X_p, x_i) \left(E_i^{PIC} - E(X_p)^{an}\right)\ ,\end{aligned}$$

where E_i^{PIC} denotes the electric field calculated by PIC at the grid point x_i and $E_i^{an}(X_p)$ the analytical electric field at the particle position X_p. Numerically, the error consists of two parts:

$$\delta\mathcal{W}_p = \delta\mathcal{W}_p^0 + \delta\mathcal{W}_p^{self}\ ,$$

the error due to the electric field E_i^0 generated by other particles in the system

$$\delta\mathcal{W}_p^0 = Q_p V_p \sum_{i=0}^{N_g} W(X_p, x_i) \left(E_i^0 - E(X_p)^{an}\right) \tag{19}$$

and the self-field

$$\delta\mathcal{W}_p^{self} = Q_p V_p \sum_{i=0}^{N_g} W(X_p, x_i) E_i^s\ ,$$

which is zero in the case of a uniform grid or a non-uniform grid with correct electric field calculation. For many-particle systems the numerical error due to particle-particle interaction is given by the superposition of the electric fields generated by the charges assigned to other grid cells

$$\delta\mathcal{W}_p^0 = \sum_{k=0}^{N_g} \delta\mathcal{W}_p^k\ ,$$

where

$$\delta\mathcal{W}_p^k = Q_p V_p \sum_{i=0}^{N_g} W(X_p, x_i)\left(E_i^k - E(X_p)^{an,k}\right) \quad . \tag{20}$$

Here the index k indicates the physical quantities generated by the charge q_k. By assuming an exact Poisson solver and extracting the self-field the electric field in 1D is given as (we assume $X_p \neq x_k$)

$$E_i^k = \begin{cases} +\frac{q_k}{\varepsilon_0}, & \text{if } k < i \\ 0, & \text{if } k = i \\ -\frac{q_k}{\varepsilon_0}, & \text{if } k > i \end{cases} .$$

For the corresponding analytical field we have

$$E(X_p)^{an,k} = \begin{cases} +\frac{q_k}{\varepsilon_0}, & \text{if } X_p > x_k \\ -\frac{q_k}{\varepsilon_0}, & \text{if } X_p < x_k \end{cases} .$$

Together with equation (20) this results in

$$\delta\mathcal{W}_p^k = \begin{cases} +\frac{Q_p V_p}{\varepsilon_0} q_k \left[W(X_p, x_k) + 2\sum_{i>k} W(X_p, x_i)\right], & \text{if } X_p < x_k \\ -\frac{Q_p V_p}{\varepsilon_0} q_k \left[W(X_p, x_k) + 2\sum_{i<k} W(X_p, x_i)\right], & \text{if } X_p > x_k \end{cases} .$$

In PIC, the weighting function gives each particle a defined size. That means $W(X_p, x_i) \neq 0$ if $x_i \in [X_p - h_p^l; X_p + h_p^r]$, where the left h_p^l and the right boundary h_p^r depends on the cell sizes next to the particle positions. For a second order weighting function like Cloud-In-Cell (CIC) [1], the particle boundaries of particle "p" with $X_p \in [x_p; x_{p+1}]$ are $h_p^l = \Delta x_{p-1}$ and $h_p^r = \Delta x_p$. If a second particle "m" with $Q_m = \sum_{i=0}^{N_g} q_i$ and $X_m \in [x_m; x_{m+1}]$ is introduced its particle boundaries are $h_m^l = \Delta x_{m-1}$ and $h_m^r = \Delta x_m$. With this set-up the numerical error in the kinetic energy due to interaction of particle "p" and "m" is given by

$$\delta\mathcal{W}_p^0 = \delta\mathcal{W}_p^m + \delta\mathcal{W}_p^{m+1}$$

$$\delta\mathcal{W}_p^0 = \begin{cases} 0, & \text{if } X_p < x_{m-1} \\ +\frac{Q_p Q_m V_p}{\varepsilon_0} W(X_m, x_m) W(X_p, x_m), & \text{if } X_p \in [x_{m-1}; x_m] \\ +\frac{Q_p Q_m V_p}{\varepsilon_0} [W(X_m, x_{m+1}) W(X_p, x_{m+1}) - W(X_m, x_m) W(X_p, x_m)], & \text{if } X_p \in [x_m; x_{m+1}] \\ -\frac{Q_p Q_m V_p}{\varepsilon_0} W(X_m, x_{m+1}) W(X_p, x_{m+1}), & \text{if } X_p \in [x_{m+1}; x_{m+2}] \\ 0, & \text{if } X_p > x_{m+2} \end{cases} .$$

Applying the following CIC weighting function for a non-equidistant grid

$$W(X_p, x_i) = \begin{cases} 1 - \frac{x_i - X_p}{\Delta x_{i-1}} & \text{for } 0 \leq x_i - X_p \leq \Delta x_{i-1} \\ 1 + \frac{x_i - X_p}{\Delta x_i} & \text{for } -\Delta x_i \leq x_i - X_p \leq 0 \\ 0 & \text{else} \end{cases} , \tag{21}$$

one gets

$$\delta\mathcal{W}_p^0 = \begin{cases} 0, & \text{if } X_p < x_{m-1} \\ \frac{Q_p Q_m V_p}{\varepsilon_0} \frac{x_{m+1} - X_m}{\Delta x_m} \frac{X_p - x_{m-1}}{\Delta x_{m-1}}, & \text{if } X_p \in [x_{m-1}; x_m] \\ \frac{Q_p Q_m V_p}{\varepsilon_0} [\frac{X_m - x_m}{\Delta x_m} \frac{X_p - x_m}{\Delta x_m} - \frac{x_{m+1} - X_m}{\Delta x_m} \frac{x_{m+1} - X_p}{\Delta x_m}], & \text{if } X_p \in [x_m; x_{m+1}] \\ \frac{Q_p Q_m V_p}{\varepsilon_0} \frac{x_m - X_m}{\Delta x_m} \frac{x_{m+2} - X_p}{\Delta x_{m+1}}, & \text{if } X_p \in [x_{m+1}; x_{m+2}] \\ 0, & \text{if } X_p > x_{m+2} \end{cases} . \tag{22}$$

An error in the kinetic energy appears only in the region where the particles are overlapping.

In PIC one simulates a large number of particles. Hence, it is important to consider the average energy error of particles of the type P in the given cell p due to interaction with other particles

$$\delta\bar{\mathcal{W}}_P = \sum_{i=0}^{N_g} \sum_{S}^{species} N_S^i \, \delta\bar{\mathcal{W}}_P^{S,i} \, . \tag{23}$$

Here, N_S^i denotes the number of particles of the type S in cell i and $\delta\bar{\mathcal{W}}_P^{S,i}$ the average energy error of particle species P at cell p due to interactions with particles of the type S in the cell i. In order to obtain $\delta\bar{\mathcal{W}}_P^{S,i}$ the average particle position can be set as

$$\bar{X}_p = x_p + 0.5\Delta x_p \, , \qquad \bar{X}_m = x_m + 0.5\Delta x_m \, .$$

Then, introducing an average velocity $\bar{V}_P^p$ from equation (22) we obtain

$$\delta\bar{\mathcal{W}}_P^{S,i} = \frac{Q_P Q_S}{4\varepsilon_0} \bar{V}_P^p \left(\delta_{m,p+1} - \delta_{m,p-1}\right) \quad ,$$

where $\delta_{i,j}$ is the Kronecker delta. Therefore, the average energy error equation (23) becomes

$$\delta\bar{\mathcal{W}}_P = \frac{Q_P \bar{V}_P^p}{4\varepsilon_0} \sum_{S}^{species} Q_S (N_S^{p+1} - N_S^{p-1}) = \frac{Q_P \bar{V}_P^p}{4\varepsilon_0} \, \delta\rho_S^p \, ,$$

where $\delta\rho_S^p = \rho_S^{p+1} - \rho_S^{p-1}$ is the gradient of the charge density of the species S. Typically $\delta\rho^i \ll \rho^i$ and the relative part of the error of energy is negligible even for a non-neutral plasma.

6 Numerical tests

In order to study effect of the modified electric field calculation on the kinetic energy different numerical tests are presented. We compare two field calculation schemes for a non-equidistant grid with an equidistant grid set-up. For an exact Poisson solver, as assumed in this work, the numerical error can only be generated by the pushing routine and by the routine calculating the electric field. The electric field acting on a particle is given by the self field E^{self} and the field E^m generated by all other particles in the system

$$E(X_p) = E^{self}(X_p) + \sum_{m=1}^{N_p} E^m(X_p) \, .$$

To separate these effects two different test set-ups are studied. In the first part, a single-particle system is used to analyses self forces. In the second part, additionally the additional influence of other charged particles is studied for a two-particle-system.

6.1 Single-particle tests

To test the modified electric field calculation scheme, a single electron with an initial non-zero velocity is studied in a 1d3v PIC code using a non-equidistant grid. A self force will appear as an artificial acceleration when crossing from small cells to larger ones and the kinetic energy will be changed.

In the code, the electron is initialized at $X_e(t=0) = 4\lambda_{D,e}$, in a domain with a length $L = 10\lambda_{D,e}$. Since the Debye length $\lambda_{D,e}$ and the plasma frequency $\omega_{p,e}$ are only defined for a many particle system, in this set up they just define an arbitrary length scale and time scale. The corresponding statistical quantities where chosen as T_e = 6 eV and $n_e = 1{\times}10^{12}\mathrm{cm}^{-3}$, defining a length scale of $\lambda_{D,e} = 1.8{\times}10^{-5}$m and a time scale of $\omega_{p,e} = 5.64{\times}10^{10}\mathrm{s}^{-1}$. The velocities are initialized to $V_e^x = \lambda_{D,e}\omega_{p,e}$ and $V_e^y = V_e^z = 0$. The non-equidistant grid consists of two parts but with individually different cell sizes. At $x = 5\lambda_{D,e}$, the cell size changes from $\Delta x_1 = 0.1\lambda_{D,e}$ to $\Delta x_2 = 5\Delta x_1$. The time step is chosen as $\Delta t = 0.002\,\omega_{p,e}^{-1}$ to guarantee sufficient time resolution of the electron dynamics.

For the Poisson solver a three point central difference scheme for the non equidistant grid

$$\frac{\phi_{i+1}\Delta x_{i-1} - \phi_i(\Delta x_{i-1} + \Delta x_i) + \phi_{i-1}\Delta x_i}{0.5(\Delta x_{i-1} \cdot \Delta x_i)(\Delta x_{i-1} + \Delta x_i)} = -\frac{1}{\varepsilon_0}\frac{\rho_i}{0.5(\Delta x_{i-1} + \Delta x_i)}$$

is applied. Here Δx_i is the length of the grid cell right to the grid point x_i which can be different from the cell size Δx_{i-1} left of x_i. For the boundary conditions $\phi_0 = 0$ and $\phi_{N_g} = (L - 2X_e)E$ are set, where E is the electric field generated by the electron. As a weighting function for particles and for the electric field the CIC for non-equidistant grid equation (21) is used.

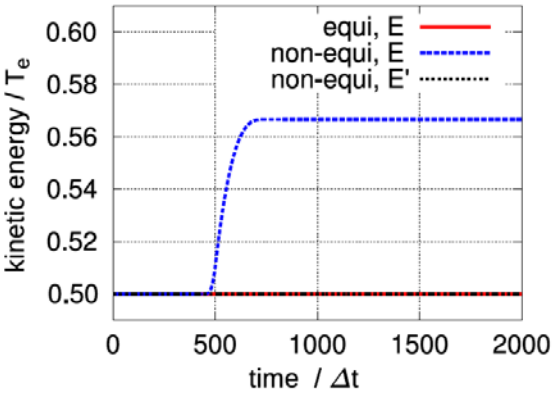

Fig. 3 Kinetic energy of one electron in its own field as a function of time, for an equidistant grid (red solid line) and a non-equidistant grid with (black dotted line) and without E-field correction (blue dashed line). The non-uniform grid boundary is reached at $t \approx 500\Delta t$.

Figure 3 shows the dependence of the electron kinetic energy as a function of time, for an E-field calculation without correction (E) and with correction (E') for a non-equidistant grid in comparison with an equidistant grid. One can clearly see that during the crossing of the grid separation boundary, the inaccurate electric field pushes the electron. This is the time period, where the weighting function W assigns the particle to grid points related to different cell sizes. Applying the modified field calculation, no increase of the electron velocity appears at the grid change and kinetic energy and momentum are conserved.

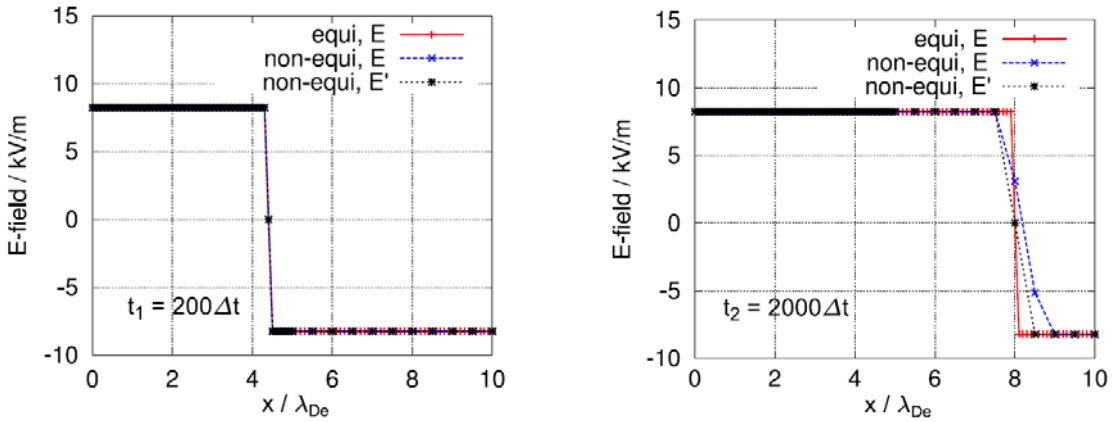

Fig. 4 Electric field as a function of x for different times. At t_1 the electron is in the part of the domain with cell size Δx_1. At t_2 the electron is in the part with Δx_2.

The simulated electric field as a function of spatial coordinate, x, is shown in Fig. 4. For $t_1 = 200\Delta t$, the electron is in the domain with grid size Δx_1 and for $t_2 = 2000\Delta t$ it is in the domain with grid size Δx_2. The difference of the electric field for t_2 between the corrected and uncorrected run in the non-equidistant grid is due to the different position of the electron. While for the corrected electric field the electron has a constant velocity, it was accelarated for the uncorrected case. The modified field calculation excludes self-forces at a cell size change and therefore conserves the momentum for a single particle.

To quantify the error in the electric field at the grid change, a second test was done. Here, the electron was initialized at the grid point $X_e(t = 0) = 5\lambda_{D,e}$ where the cell size changes. Its velocity was initialized to

$\mathbf{V}_e = \mathbf{0}$. According to the analytic solution, the electric field has to be zero at X_e. The calculated electric field as a function of the coarsening of the cell size can be seen in Fig. 5.

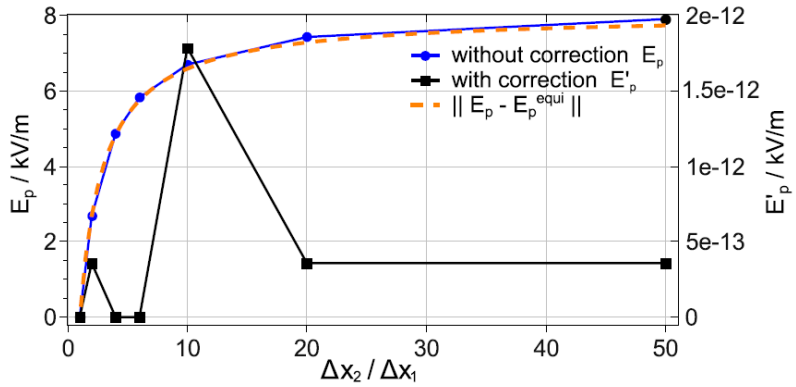

Fig. 5 Error of the electric field calculation for one electron located at the grid change with initial velocity $\mathbf{V} = \mathbf{0}$.

The error for the corrected field is in the range of the numerical error, while the error of the uncorrected electric field increases with grid coarsening and saturates. For the uncorrected electric field, the error related to the equidistant grid can be derived as

$$||E_p - E_p^{equi}|| \;=\; ||\frac{\phi_{p-1} - \phi_{p+1}}{\Delta x_1 + \Delta x_2} - \frac{\phi_{p-1}^{equi} - \phi_{p+1}^{equi}}{2\Delta x_1}|| \;=\; \frac{\Delta x_2 - \Delta x_1}{\Delta x_1 + \Delta x_2}\,||E||$$

with the $\phi_{p-1} = \phi_p + E \cdot \Delta x_1,\ \phi_{p+1} = \phi_p + E \cdot \Delta x_2$ and $\phi_{p\pm1}^{equi} = \phi_p + E \cdot \Delta x_1$ for the equidistant grid. The error estimate is shown in Fig. 5 as an orange dashed line. It agrees with the measured field. For a coarser grid, Δx_2 decreases and reduces the influence of Δx_1. The error of the field calculation saturates with

$$\lim_{\Delta x_2 \to \infty} ||E_p - E_p^{equi}|| = ||E|| \,.$$

The same error estimate for the corrected electric field gives

$$||E'_p - E_p^{equi}|| \;=\; ||\frac{\phi_{p-1} - \tilde{\phi}}{\Delta x_1 + \Delta x_2} - \frac{\phi_{p-1}^{equi} - \phi_{p+1}^{equi}}{2\Delta x_1}|| \;=\; 0$$

with the interpolated potential $\tilde{\phi} = \phi_p \frac{\Delta x_2 - \Delta x_1}{\Delta x_2} + \phi_{p+1} \frac{\Delta x_1}{\Delta x_2}$.

6.2 Two-particle test

For a more realistic test-case the interaction of different particles has to be taken into account. We consider a two-particle system: one electron interacting with a singly charges Argon ion. Both particles are initialized with zero velocity, so that the total momentum $p_{tot} = 0$. The simulation domain has a length of $L = 10\lambda_{D,e}$ as for the single-particle tests. For the equidistant grid, the domain has a cell size of $\Delta x = 0.1\lambda_{D,e}$. In the non-equidistant grid a change in cell size from $\Delta x_1 = \Delta x$ to $\Delta x_2 = 2\Delta x_1$ is implemented at $5\lambda_{D,e} = 50\Delta x_1$. In order to place the zone of particle interaction near the change of cell size, the ion is initialized at $X_i(t = 0) = 49.5\Delta x_1$. The initial position of the electron is taken at $X_e(t = 0) = 39.0\Delta x_1$. While the ion is nearly "frozen" and does not leave its cell, the electron is oscillating around the ion and therefore crosses the grid change frequently. The time step was chosen according to the average velocity of the ion $\bar{V}_e = 8.3{\times}10^4$m/s and the minimum cell size Δx_1: $\Delta t = \delta t \cdot \frac{\Delta x_1}{\bar{V}_e}$, where $\delta t = 8.1{\times}10^{-5}$ is a small dimensionless parameter. During the total calculation time of $t_{max} = 10^5 \Delta t$, the electron oscillates 1.2 times around the ion. The same Poisson solver and the weighting function where used, as in section 6.1. The following boundary conditions have been set: $\Phi(x = 0) = \Phi(x = 10\lambda_{D,e}) = 0$.

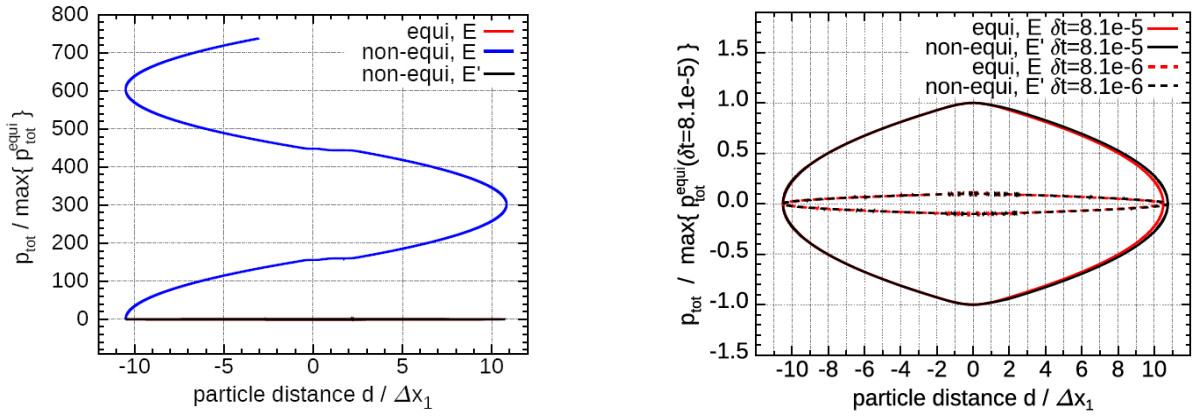

Fig. 6 Total momentum of a two particle system as a function of the particle distance, for an equidistant and a non-equidistant grid with and without E-field correction.

In Figure 6, the total momentum is shown for three cases: equidistant grid, non-equidistant grid and non-equidistant grid with corrected field calculation. It is given normalized to the maximum momentum of the equidistant grid $max\{p_{tot}^{equi}\}$ = 5.1×10^{-28}kg m/s as a function of the distance between particles normalized to Δx_1. The total momentum of the uncorrected non-equidistant grid is continuously increasing (see the left figure), as consequence of the wrong electric field, continuously acting on the ion. For this scheme, the momentum is not conserved. In comparison, the equidistant grid as well as the non-equidistant grid with the corrected field calculation have a total momentum much closer to the analytical value of $p_{tot} = 0$.

For a better comparison, both cases are shown as solid lines at the right hand side in Fig. 6. In dotted lines, the total momentum is given for a 10 times smaller time step $\delta t = 8.1\times10^{-6}$. All curves are closed ellipses, therefore the momentum is conserved during the 1.2 oscillations. For both grids the the thickness of the ellipses decreases with the 10 times smaller time step by a factor of 10 and is therefore determined by the numerical error of the solver due to the chosen time step Δt. For the non-equidistant grid a deviation is visible for both time steps, if the electron is located in the coarser grid ($d > 0.5\Delta x_1$). Here, the total momentum is larger than in the equidistant grid. This implies that this error is caused by the numerical error of the solver routine due to the coarser cell size. But it does not affect the conservation of momentum.

As shown in section 5, an error in the kinetic energy appears only in the region where the particles are overlapping. This "overlapping zone" has an extend of 3 grid cells and can be seen in Fig. 7 for $|d| \leq 1.5\Delta x_1$. In this simulation the ion was placed in the middle of the cell with a distance of 4 cells from the non-uniform cell boundary. Other parameters were: $X_i(t=0) = 50.5\Delta x_1$, $X_e(t=0) = 40.0\Delta x_1$, change of cell size at $56\Delta x_1$ from Δx_1 to $\Delta x_2 = 2\Delta x_1$. The total kinetic energy is calculated by the sum of the measured kinetic energy and potential energy

$$\mathcal{E}_{tot}(t) = \mathcal{W}(t) + \mathcal{U}(t) = \sum_{p=1}^{N_p} \frac{m_p \bar{\mathbf{V}}_p(t)}{2} + \sum_{p=1}^{N_p} q_p E(X_p(t)) \quad .$$

For the Boris pusher used in this 1D simulation, the velocities are calculated at half time steps. Therefore, the kinetic energy is calculated from the average velocity

$$\bar{\mathbf{V}}_p(t) = 0.5 \cdot (\mathbf{V}_p(t - 0.5\Delta t) + \mathbf{V}_p(t + 0.5\Delta t)) \, .$$

For the potential energy of the particles, the electric field at the particle position is calculated by

$$E(X_p(t)) = \sum_{i=0}^{N_g} W(x_i, X_p) E_i - C(x_i, X_p) \quad ,$$

where the function $C(x_i, X_p)$ is a correction of the electric field at particle position. It is necessary due to the fact, that the electric field is given only at grid points and therefore is varying with respect to the distance to the

next grid point. For a two particle system with the CIC shape function (21) it is given by

$$C(x_i, X_p) = \frac{Q_p^2}{\varepsilon_0} \frac{(X_p - x_i)(x_{i+1} - X_p)}{\Delta x_i^2} .$$

For the 1D PIC, it can be shown that the calculated potential gives the correct analytical value.

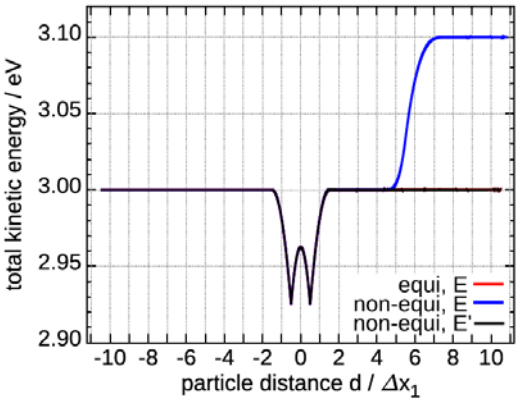

Fig. 7 Total kinetic energy as a function of the particle distance.

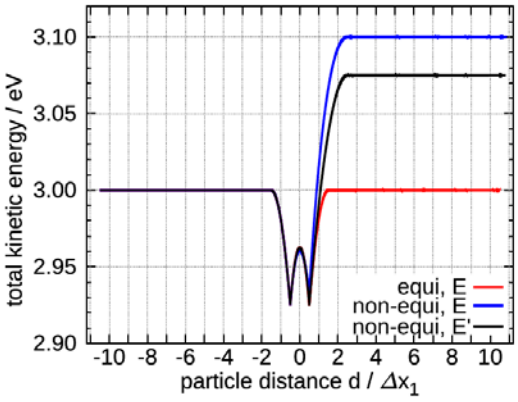

Fig. 8 Total kinetic energy as a function of the particle distance. The change of the cell size is next to the ion.

As expected, the uniform and non-uniform mesh with correct electric field calculation produces the same error. According to equation 22 the error changes sign when the electron "crosses" the ion, so that the total error after 1.5 cells is zero. If the ion is not placed in the middle of the cell then the positive and negative contributions are different and a residual error appears. This error is known [7] and corrected in many particle systems due to averaging over the particles, as described in section 5. Additional collisions will reduce it further. Contrary to this, the uncorrected code produces an error when the electron crosses the non-uniform boundary due to self forces.

More critical is the case when the ion is placed next to the non-uniform cell boundary. Also in this case the ion is placed in the middle of the cell with the size Δx_1 and to the left a cell with size $\Delta x_2 = 2\Delta x_1$. The total kinetic energy as a function of the particle distance is given in Fig. 8. For all three cases, equidistant grid, non-equidistant grid with and without field correction, the error in energy is different. The equidistant case is similar to the one shown in Fig. 7. Contrary to this, the non-equidistant case with the field correction produces a residual error caused by the fact that the cell sizes from the left and right hand side of the ion are different and the positive and negative errors do not cancel each other (equation 22). In the case of the non-equidistant grid without field correction the error is larger. This is a consequence of a self-force.

As shown in section 5, in many particle systems the error in the corrected electric field calculation even for a non-neutral plasma is negligible due to averaging over the particles. Hence, the PIC model with an non-equidistant grid and corrected electric field conserves the average energy with a high accuracy.

7 Conclusions and discussion

In this work effects of non-equidistant grids on momentum and kinetic energy conservation was studied for simple test cases of an electrostatic 1D PIC code. Since an exact Poisson solver was assumed only numerical errors concerning the particle pusher were analysed. For a standard central difference scheme for electric field calculation, generation of artificial electric fields at the particle position was shown if the particle is situated next to a change of cell size. This generates a self force. With the help of a Green's function theory it was proven that this destroys momentum conservation. To reduce this error a modified electric field calculation scheme was derived.

For non-equidistant grids violation of kinetic energy conservation independent of the electric field calculation scheme was found for a two-particle system. For many particles, it was shown that for an average over all

particles in one cell the error scales with the charge density gradient in the three surrounding cells, which is usually negligible.

To test the accuracy of the two electric field calculation schemes numerical tests were done to compare the results with an equidistant grid set-up. All tests showed an improved momentum and kinetic energy conservation for the modified calculation scheme of the electric field. In a first test system only the effects of the self force was studied with respect to momentum conservation. Here, analytical estimates were confirmed. In a second numerical test system the influence of electric fields generated by other particles in the system was investigated. For this case with two particles momentum conservation and a violated kinetic energy conservation in the so called "overlapping zone" of the particles was shown in agreement with the analytical results.

The presented electric field calculation scheme can be derived in the same way for Cartesian coordinates in higher dimensions. But although numerical errors due to the particle pusher are reduced, for many particle systems an exact Poisson solver is not ensured.

Acknowledgements This work was supported by the German Space Agency DLR through Project 50 RS 1101. This work of D. Tskhakaya was supported by EURATOM and carried out within the framework of the European Fusion Development Agreement. The views and opinions expressed herein do not necessarily reflect those of the European Commission.

References

[1] R. Hockney and J. Eastwood, "Computer simulation using particles", Adam Hilger 1981.
[2] C.-D. Munz, R. Schneider, E. Sonnendrücker et al., International Journal for Numerical Methods in Engineering **44**, 461 (1999).
[3] G. Lapenta, "Automatic adaptive multi-dimensional particle-in-cell", Advanced Methods for Space Simulations, p. 61 2007.
[4] T. Westermann, Journal of Computational Physics **101**, 307-313 (1992). doi:10.1016/0021-9991(92)90008-M
[5] C.A. Fichtl, "An Arbitrary Curvilinear Coordinate Particle In Cell Method", Ph.D. thesis, Nuclear Engineering, University of New Mexico 2010.
[6] P. Colella and P.C. Norgaard, Journal of Computational Physics **229**, 947-957 (2010). doi:f10.1016/j.jcp.2009.07.004g
[7] D. Tskhakaya, K. Matyas, R. Schneider et al., Contrib Plasma Phys. **47**, 563-594 (2007).